ELSEVIER

Thermochimica Acta 262 (1995) 215–226

thermochimica
acta

# Temperature-programmed reaction and *in situ* infrared study of CO adsorbed on $Rh/SiO_2$ and $Ag–Rh/SiO_2$ catalysts

R. Krishnamurthy, S.S.C. Chuang*

*Department of Chemical Engineering, The University of Akron, Akron, OH 44325-3906*

Received 30 September 1994; accepted 18 March 1995

## Abstract

The temperature-programmed reaction (TPR) technique coupled with infrared (IR) spectroscopy has been employed to study the reactivity of adsorbed CO towards hydrogen. The combination of the two techniques provides information on the structure and reactivity of adsorbates, activation energy and kinetic data for the CO hydrogenation reaction. CO adsorption on $Rh/SiO_2$ at 298 K produced mainly linear and bridged CO on the surface. Linear CO appears to be more reactive than bridged CO in the formation of methane during TPR over $Rh/SiO_2$. The addition of silver to $Rh/SiO_2$ promotes the formation of gem-dicarbonyl CO and suppresses the formation of bridged CO during CO adsorption at 298 K. The disproportionation of gem-dicarbonyl CO and the reduction of $Rh^+$ by oxidation of the CO ligand of $Rh^+(CO)_2$ produce CO, $CO_2$, and surface carbon on the $Ag–Rh/SiO_2$ catalyst at temperatures above 310 K. Hydrogenation of surface carbon begins at 390 K leading to methane formation. The methane peak temperature was observed at 442 K on the $Ag–Rh/SiO_2$ and at 420 K on $Rh/SiO_2$. The higher hydrogenation temperature of adsorbed CO and surface carbon over $Ag–Rh/SiO_2$ as compared to $Rh/SiO_2$ is attributed to the suppression of hydrogenation by Ag.

*Keywords:* Adsorption; CO hydrogenation; *In situ* infrared spectroscopy; Reactivity; Temperature-programmed reaction

## 1. Introduction

Temperature-programmed reaction is a thermoanalytical technique for obtaining information on the kinetics and reaction mechanism on a catalyst surface [1,2]. TPR

---

* Corresponding author.

*SSDI* 0040-6031(95)02382-8

involves the surface-catalyzed reaction of an adsorbate with a reactive gas or the reaction between co-adsorbates under a controlled heating rate. Mechanistic and kinetic information can be obtained from the peak maximum and the shapes of peaks of the desorption profile for the products and unreacted reactants. Because of the transient nature of the TPR experiment where both temperature and surface coverage vary with time, it provides important reaction information which is not available from steady-state kinetic measurements. However, the chemical identity of the adsorbates leading to the TPR profile of the products and unreacted reactants cannot be obtained from this technique. Fourier transform infrared spectroscopy (FTIR) permits *in situ* determination of the structure and coverage of adsorbates in a wide range of conditions. Although TPR and FTIR have been extensively used in the investigation of adsorption, surface reaction, and desorption in heterogeneous catalysis, simultaneous use of these two techniques has rarely been reported [3–5].

CO hydrogenation has been the subject of extensive studies because of its importance in the formation of hydrocarbons and oxygenated products with a wide variety of applications [6–11]. CO hydrogenation over Rh-based catalysts has been studied extensively because of their unique activity and selectivity for synthesis of oxygenates. The adsorption of CO on the supported Rh surface produces linearly adsorbed, bridge-bonded, and gem-dicarbonyl CO [11–17]. Different forms of adsorbed CO could exhibit different reactivities towards product formation.

Temperature-programmed reaction and separate infrared (IR) studies conducted by Fujimoto et al. have suggested bridged CO to be the active species for methanation over $Rh/Al_2O_3$ catalysts [18]. In contrast, pulse surface reaction rate analysis (PSRA) studies indicate linear CO to be responsible for methanation over $Rh/Al_2O_3$ [19] and $Ru/Al_2O_3$ [20] catalysts. Solymosi and coworkers, using a flow technique and separate IR studies on supported Rh catalyst, have suggested that the dissociation of linear CO occurs in the presence of $H_2$ or $H_2/CO$ mixture through the formation of Rh-carbonyl-hydride species [21,22]. Although the binding energy of linear CO was greater than that of bridged CO on Rh (111) single crystals [23], while the linear CO binding energy was less than that of bridged CO on Ni (111) single crystals [24], the site for CO dissociation and the type of adsorbed CO involved in CO hydrogenation on the metal surface remain unclear.

The objective of this work was to study the reactivity of different forms of adsorbed CO towards hydrogen for methanation and the effect of Ag on the various forms of adsorbed CO, using an *in situ* infrared technique coupled with TPR. Our previous studies have shown that silver blocks the bridged CO sites [11,25]. Investigation of the reactivity of different forms of adsorbed CO on $Rh/SiO_2$ and $Ag$-$Rh/SiO_2$ catalysts should reveal the role of adsorbed CO in the methanation reaction. The change in the intensities of adsorbed CO and the rate of methane formation during the TPR study were monitored by FTIR and a mass spectrometer, respectively. Results of this study demonstrate the usefulness of simultaneous FTIR and TPR measurement in obtaining information on the structure and reactivity of adsorbates, the reaction mechanism, and the activation energy of reaction.

## 2. Experimental

### 2.1. Catalyst preparation

A 3 wt% $Rh/SiO_2$ catalyst was prepared by impregnation of large-pore silica (Strem Chemicals, 300 $m^2/g$) using rhodium nitrate ($Rh(NO_3)_3 \cdot 2H_2O$) solution. The ratio of solution to weight of support material was 1 $cm^3$ to 1 g. Supported Ag–Rh catalyst, with a molar ratio of Ag to Rh of 1, was prepared by coimpregnation of silver and rhodium nitrate solutions. The catalysts were dried in air overnight at 313 K after impregnation and then reduced in a 20 $cm^3 min^{-1}$ flow of hydrogen at 673 K for 16 h. The details of the characterization are reported elsewhere [11]. The Rh crystallite size on the $Rh/SiO_2$ catalyst was determined by X-ray diffraction line-broadening as 87 Å. The crystallite sizes of Rh and Ag on the $Ag–Rh/SiO_2$ catalyst were 136 and 395 Å, respectively. The amount of hydrogen chemisorbed measured by the flow chemisorption technique was found to be 39.2 μmol $(g\ cat)^{-1}$ for $Rh/SiO_2$ and 5.4 μmol $(g\ cat)^{-1}$ for $Ag–Rh/SiO_2$ catalyst. The catalyst was pressed into a self-supporting disk and then placed in the IR cell and reduced *in situ* at 673 K before TPR studies.

### 2.2. TPR studies

A schematic of the integrated infrared-mass spectrometric system is shown in Fig. 1. The IR cell is made of stainless-steel tubing with two $CaF_2$ windows. The design of the

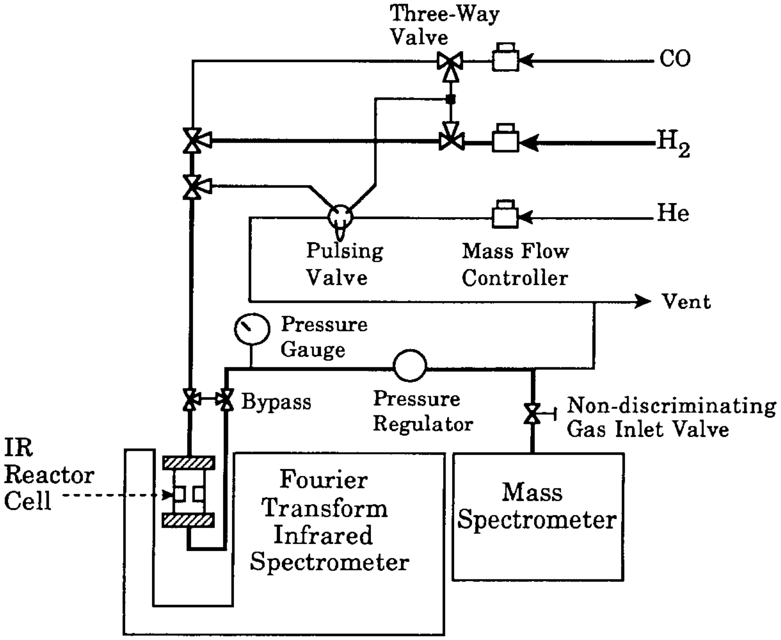

Fig. 1. Schematic diagram of the experimental apparatus used for the combined IR and TPR studies.

IR cell is reported elsewhere [26]. The catalyst is pressed in the form of a disk and placed in the center of the reactor with the tip of a thermocouple touching the disk for accurate measurement of the catalyst temperature. Two $CaF_2$ rods are placed between the catalyst disk and the $CaF_2$ windows to minimize the dead space and to reduce the optical path length for the gases within the reactor. The IR cell is capable of operating up to 723 K and 6.0 MPa.

Carbon monoxide was introduced into the IR cell to adsorb on the catalyst surface at 298 K and 0.1 MPa and the gas phase CO was removed by flowing He through the reactor. The TPR was conducted in a 55 $cm^3 min^{-1}$ flow of 9.1% $H_2$ in He at a ramping rate of 20 $K min^{-1}$ from 298 K to 673 K and held at 673 K for 15 min. The hydrogen, due to its ease of ionization, is diluted with helium to control the vacuum in the ionization chamber of the mass spectrometric system. IR spectra during the TPR were recorded by an FTIR spectrometer with a DTGS detector at 4 $cm^{-1}$ resolution. The gaseous effluent from the IR reactor was monitored by a Balzers QMG 112 mass spectrometer (MS) equipped with a non-discriminating gas inlet valve which yields rapid response and excludes mass discrimination. The species monitored by the MS were methane ($m/e = 15$), carbon monoxide ($m/e = 28$), carbon dioxide ($m/e = 44$), and water ($m/e = 18$). Other species such as $C_2H_6$, $C_2H_5OH$, and $CH_3CHO$ were not observed. The intensity units obtained from the MS signal on the ordinate of the TPR plots were divided by the response factor for each species to give the rate of desorption and product formation of each species. Calibration for obtaining the response factor was performed just before the TPR studies under identical flow and vacuum conditions for the MS as those used during the TPR. Determination of the response factor of a species involves injecting a known amount of the species into a helium flow through the bypass and measuring its MS response as a function of time. The ratio of area under the response curve to the number of moles of species injected gives the response factor for the species. Due to the strong tendency of water to adsorb on the walls of the transportation lines and the MS chamber, it is difficult to obtain the response factor for water. Thus, the $H_2O$ profile in Figs. 3 (p. 6) and 5 (p. 8) provide only qualitative information.

## 3. Results and discussion

Fig. 2 shows the IR spectra of CO adsorbed on the $Rh/SiO_2$ catalyst during TPR with hydrogen. The IR spectra of adsorbed CO at 298 K and 0.1 MPa of CO followed by the removal of gaseous CO show a linear CO band at 2058 $cm^{-1}$, a bridged CO band at 1870 $cm^{-1}$, and weak gem-dicarbonyl bands at 2097 and 2027 $cm^{-1}$. Two co-added scans collected during the TPR yielded infrared spectra with low signal-to-noise (s/n) ratio. Increasing the number of co-added scans increases the time for collection of IR spectra which results in the loss of transient information during the TPR. A switch from pure He flow to a mixture of $H_2$ in He flow did not result in any change in the intensity of the adsorbed CO. An increase in reactor temperature caused a decrease in the intensity and wavenumber of both linear and bridged CO; the rate of decrease in intensity varied with temperature. The decrease in the wavenumber of

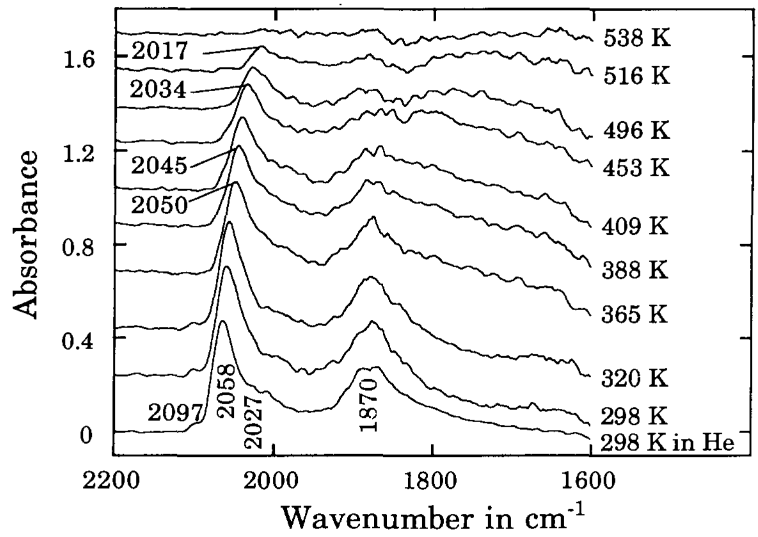

Fig. 2. Infrared spectra of the temperature-programmed reaction of CO adsorbed on $Rh/SiO_2$.

linear and bridged CO with a decrease in their intensities is due to the reduction in dipole–dipole coupling as a result of low coverage of adsorbed CO [27]. The low wavenumber of linear CO could also be due to the attachment of hydrogen on the linear CO site to form Rh–carbonyl-hydride. However, no direct evidence is obtained to support the presence of Rh–carbonyl-hydride during TPR studies.

The major gas phase products resulting from TPR include CO, $CH_4$, $H_2O$, and $CO_2$, whose TPR profiles are shown in Fig. 3. The $CO_2$ profile exhibited a very weak band from 317 to 416 K and is a minor product of the reaction. The gas phase CO profile from the effluent of the IR cell shows a desorption peak at about 366 K. The intensity of linear CO decreased more rapidly than that of bridged CO in the temperature range 320–365 K where gaseous CO and $CO_2$ were observed. Although it is not possible to distinguish the type of adsorbed CO that forms gaseous CO or $CO_2$, most of the linearly adsorbed CO appears to desorb as gaseous CO in this temperature range.

The absence of CO profiles at temperatures above 435 K reveals that all the adsorbed CO present above 435 K was either dissociated to surface carbon and oxygen or converted to methane. The oxygen generated from the dissociation of CO combined primarily with hydrogen to yield water, and the reaction of this oxygen with the undissociated CO to form $CO_2$ did not occur to a significant extent. The rapid decrease in the linear CO intensity corresponds to the methane peak at 420 K. This result suggests that the linear CO is more reactive than bridged CO toward hydrogen, leading to methane formation, provided that rapid exchange between linear and bridged CO does not occur. All the adsorbed CO disappears from the surface at temperatures above 516 K, as shown in Fig. 2. A rapid decrease in the intensity of linear and bridged CO is observed corresponding to the appearance of the tailing methane peak in the range 470–516 K. The presence of the tailing methane shoulder between 516 and 555 K may

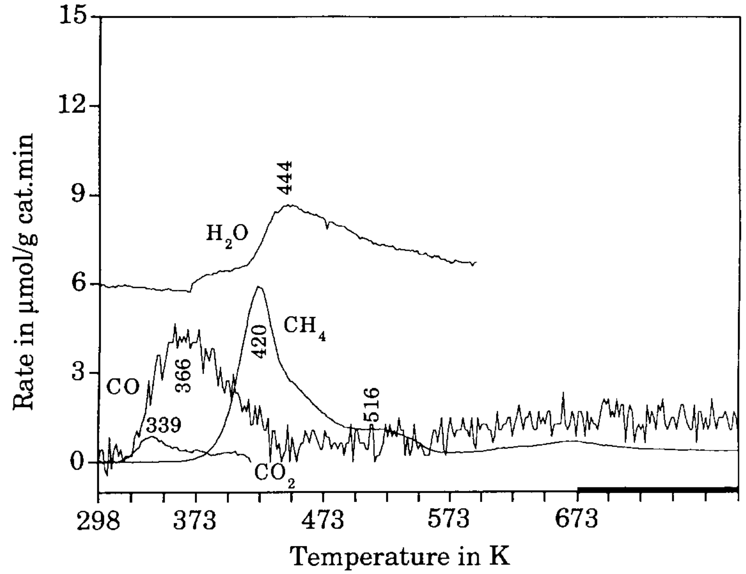

Fig. 3. TPR product response for $Rh/SiO_2$.

be due to the hydrogenation of the surface carbon remaining on the catalyst surface. The hydrogenation of surface carbon to methane occurred at a higher temperature than the hydrogenation of surface oxygen to form water which began at 367 K with a peak at 444 K. It should be noted, however, that the water response obtained could also be partly due to the readsorption and the desorption of water adsorbed on the walls of the heated transportation lines and the heated chamber of the MS system. Hence, the information obtained from water response cannot be used to elucidate the reaction mechanism.

The IR spectra of CO adsorbed on $Ag–Rh/SiO_2$ catalyst during TPR is shown in Fig. 4. The IR spectra of adsorbed CO at 298 K and 0.1 MPa of CO in a flow of He through the reactor show a linear CO band at 2063 $cm^{-1}$, a weak bridged CO band at 1853 $cm^{-1}$, the symmetric vibration of gem-dicarbonyl band at 2095 $cm^{-1}$, and a weak shoulder at 2036 $cm^{-1}$ due to asymmetric vibration of gem-dicarbonyl. The formation of gem-dicarbonyl suggests the presence of isolated $Rh^+$ sites on $Ag–Rh/SiO_2$. This is in agreement with our previous observation for CO adsorption on the same catalyst [11]. The higher intensity of gem-dicarbonyl on Ag–Rh as compared to that of gem-dicarbonyl on $Rh/SiO_2$ suggests that the presence of Ag promotes the formation of $Rh^+$ sites at 298 K. XPS studies at 303 K revealed the presence of $Rh^+$ sites on $Ag\text{-}Rh/SiO_2$ after hydrogen reduction at 513 K [11]. The transfer of a high net electron density is suggested to occur between Rh and Ag at low silver coverages [28]. It is difficult to conclude with the available information whether such an electron transfer does occur on our catalyst. The increase in concentration of surface $Rh^+$ on Ag–Rh may also be due to the promotion of disruption of Rh crystallites by Ag in the presence of CO at 298 K. $H_2$ chemisorption and XRD measurement show that $Ag–Rh/SiO_2$

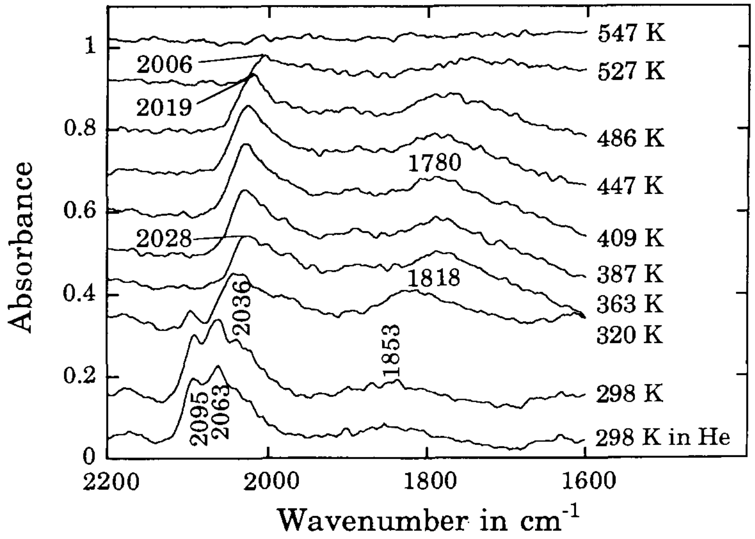

Fig. 4. Infrared spectra of the temperature-programmed reaction of CO adsorbed on Ag–Rh/$SiO_2$.

possesses large Rh crystallites with an average size of 136 Å. *In situ* XRD of the Ag–Rh catalyst is required to determine whether Ag promotes Rh disruption in CO atmosphere.

Increasing the temperature caused an initial decrease and then a slight increase in the linear CO intensity. A small increase in the intensity of the bridged CO band and a decrease in the intensity of the gem-dicarbonyl bands were also observed with increase in temperature. The slight growth in the linear and bridged CO bands suggests the occurrence of reductive agglomerations of $Rh^+$ sites leading to the formation of reduced Rh crystallites which adsorb linear and bridged CO [15, 29]. Reductive agglomeration may cause the aggregation of Ag atoms at the expense of the interdispersed Ag atoms on the Rh crystallites. The aggregation of the Ag atoms on the Rh surface due to reactant-induced surface reconstruction has also been observed under CO hydrogenation conditions (513 K) which results in a decrease in the ratio of the intensity of linear to bridged CO [12].

The major gas-phase products resulting from the TPR on Ag–Rh/$SiO_2$ catalyst include CO, $CH_4$, and $CO_2$ whose TPR profiles are shown in Fig. 5. Both gaseous CO and $CO_2$ peaks were observed in the temperature range 310–375 K, where gem-dicarbonyl bands show a rapid decline in intensity. Linear and bridged CO appear to play little role in $CO_2$ formation and desorption as gaseous CO in this temperature range as both species show little variation in their intensities. The formation of the $CO_2$ peak could be due to either (i) disproportionation of gem-dicarbonyl CO, or (ii) the reduction of $Rh^+$ [$2Rh^+(CO)_2 + O^{-2} \rightarrow (Rh)_2 - CO + CO_2 + 2CO$, where $O^{-2}$ is an oxygen of the surface oxide and $(Rh)_2 - CO$ is the bridged CO] by oxidation of a CO ligand of $Rh^+(CO)_2$ [30]. The oxidation of CO ligand would lead to the simultaneous formation of CO and $CO_2$ in the stoichiometric ratio of 2 to 1. The slight difference in

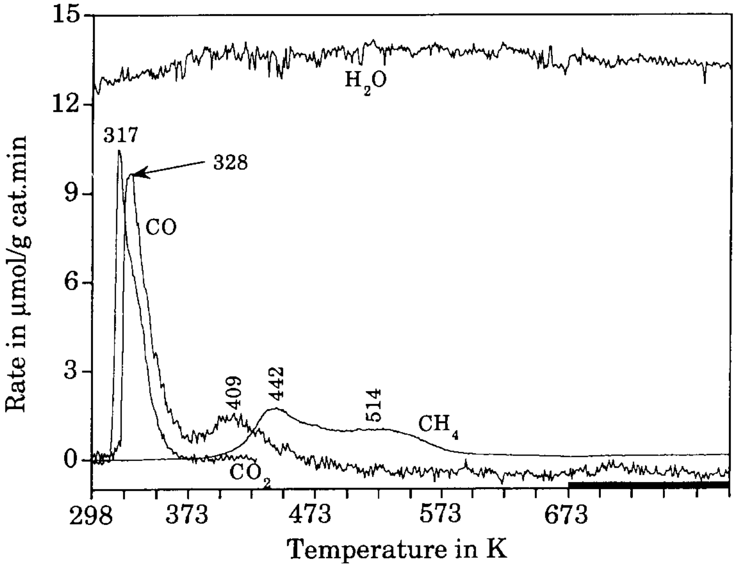

Fig. 5. TPR product response for Ag-Rh/$SiO_2$.

peak temperatures exhibited by CO and $CO_2$ suggests that the reduction of $Rh^+$ by oxidation of a CO ligand of $Rh^+(CO)_2$ may occur to some extent. Such a reduction process can also result in the formation of reduced Rh crystallites which chemisorb linear and bridged CO. The area under the CO peak at 328 K corresponds to 13.7 μmol of CO, and the area under the $CO_2$ peak at 317 K corresponds to 10.0 μmol of $CO_2$, calculated after accounting for the response factors for CO and $CO_2$ on the mass spectrometer. The ratio of formation of CO to $CO_2$ in the temperature range 310–375 K is not in the expected stoichiometric ratio of 2 to 1 which suggests that part of the $CO_2$ probably resulted from the disproportionation of gem-dicarbonyl. CO disproportionation has also been found to be the major pathway for $CO_2$ formation from $Rh^+(CO)_2$ on $RhCl_3/SiO_2$ [31].

The methane peak at 442 K results from the hydrogenation of surface carbon which is produced from the CO disproportionation reaction as discussed above. The lack of contribution of both linear and bridged CO to the $CH_4$ peak is evidenced by little change in the intensity of linear and bridged CO at temperatures around 442 K where the methane peak was formed. A rapid decrease observed in the intensities of both linear and bridged CO corresponds to the tailing methane shoulder in the range 494–593 K.

The effect of Ag on the CO adsorption and the reactivity of various forms of adsorbed CO for methanation can be elucidated from a comparison of the IR and TPR results of both Rh and Ag–Rh catalysts. The addition of silver promotes the formation of gem-dicarbonyl, $Rh^+(CO)_2$, as shown by the IR spectra for Ag–Rh/$SiO_2$ in Fig. 4. Although the gem-dicarbonyl can be dissociated to surface carbon via the disproportionation reaction in the range 298–340 K during TPR, its role in CO dissociation over

Ag-Rh/$SiO_2$ could be very limited under steady-state reaction conditions (513–573 K). The reductive agglomeration of $Rh^+$ sites by CO and $H_2$ in the temperature range 513–573 K under steady-state reaction conditions prevents the formation of gem-dicarbonyl and diminishes the $Rh^+$ sites [11].. Only linear and bridged CO were observed on the surface under CO hydrogenation conditions at temperatures above 513 K [11].

Ag has little effect on the reactivity of bridged CO on Rh/$SiO_2$. A rapid decrease in the bridged CO intensity on the Rh/$SiO_2$ catalyst was observed in the range where the tailing methane peak was observed. A rapid decline in the intensity of the bridged CO species accompanied by the formation of methane was also observed on Ag–Rh/$SiO_2$ at about the same temperature at which the tailing methane peak was observed on Rh/$SiO_2$. The low wavenumber of bridged CO on Ag–Rh/$SiO_2$ compared to that of the bridged CO on Rh/$SiO_2$ is due to a decrease in dipole–dipole interaction as a result of low surface coverage of bridged CO on Ag–Rh/$SiO_2$.

Ag suppresses the hydrogenation of the surface carbon species generated from linear and gem-dicarbonyl CO on Ag–Rh/$SiO_2$ as shown by the higher methane peak temperature on Ag–Rh/$SiO_2$ than on Rh/$SiO_2$. Ag probably limits the access of linear CO and carbon to the $H_2$ which results in a slower decrease in the intensity of linear CO and a shift in methane peak temperatures on Ag–Rh/$SiO_2$. TPR studies on catalysts with Ag to Rh ratios of 0.25 and 0.5 also showed a progressive increase in the $CH_4$ peak temperature with increase in Ag content. The suppression of methanation brought about by Ag has been observed for CO hydrogenation over an Ag–Rh (111) single crystal surface where Ag is found to geometrically block methanation sites on a one-to-one basis [32].

A comparison of peak temperatures and the amount of product desorbed for Rh/$SiO_2$ and Ag–Rh/$SiO_2$ is summarized in Table 1. The methane peak temperatures of the TPR profile provide an estimate of the rate constant for methanation. The activation energies for the methanation reaction can be estimated by using the half-widths of the methane peaks obtained during the TPR [33]. The tail in the methane peaks of Rh/$SiO_2$ and Ag–Rh/$SiO_2$ catalysts was not considered in the calculation of activation energy. The activation energy calculated is for the hydrogenation of linear CO on Rh/$SiO_2$ catalyst and that of surface carbon on the Ag–Rh/$SiO_2$

Table 1
Peak temperature and amounts of product desorbed during TPR over Rh/$SiO_2$ and Ag–Rh/$SiO_2$ catalysts

| | Rh/$SiO_2$ | | Ag–Rh/$SiO_2$ | |
|---|---|---|---|---|
| | Peak temperature/K | Amount of product formed during TPR/ μmol (g cat)$^{-1}$ | Peak temperature/K | Amount of product formed during TPR/ μmol (g cat)$^{-1}$ |
| CO | 366 | 15.1 | 328 | 13.7 |
| $CO_2$ | 339 | 2.1 | 317 | 10.0 |
| $CH_4$ | 420 | 16.9 | 442 | 7.8 |

Table 2
Activation energy and rate constant for methanation during TPR over $Rh/SiO_2$ and $Ag–Rh/SiO_2$ catalysts

| Catalyst | $H_2$ chemisorption/ μmol (g cat)$^{-1}$ | Peak temperature/ K | Half-width/ K | Activation energy/ kJ mol$^{-1}$ | Rate constants$^{-1}$ |
|---|---|---|---|---|---|
| $Rh/SiO_2$ | 39.2 | 420 | 38 | 129.5 | $2.3 \times 10^{16}$ |
| $Ag–Rh/SiO_2$ | 5.4 | 442 | 50 | 107.6 | $9.0 \times 10^{12}$ |

catalyst. The relation used for the calculation of activation energies is as follows

$$\frac{E_d}{RT_p} = 2\left[-1 + \left(1 + \frac{3.117 T_p^2}{W_{1/2}^2}\right)^{1/2}\right]$$

where, $E_d$ is the activation energy, J/mol
$R$ is the Universal gas constant, J/mol K
$T_p$ is the peak temperature, K, and
$W_{1/2}$ is the half-width of the peak.

Shape index and curve symmetry parameters were calculated for the methane response as described by Ibok and Ollis [34] and Chen [35]. These results indicate that the methanation reaction during the TPR studies followed second-order kinetics in the absence of readsorption. The absence of readsorption in this study was confirmed by the low ratio of adsorption rate to the carrier gas flow rate [36]. The peak temperatures, half-widths, and activation energy values for $Rh/SiO_2$ and $Ag–Rh/SiO_2$ catalysts are summarized in Table 2. The values for activation energies calculated from peak-width analysis methods are in fairly good agreement with activation energies calculated from the reaction rates obtained during steady-state reaction studies for both catalysts [37]. Rate constants calculated at 513 K from these kinetic parameters indicate that the methanation activity for $Rh/SiO_2$ catalyst is much higher than that for $Ag–Rh/SiO_2$ catalyst.

## 4. Conclusions

The effect of Ag addition on $Rh/SiO_2$ for hydrogenation of CO can be summarized as follows.

(1) Silver promotes the formation of gem-dicarbonyl and suppresses the formation of bridged CO on $Rh/SiO_2$.
(2) Gem-dicarbonyl reacts to form $CO_2$, CO, and surface carbon at temperatures above 310 K on the $Ag–Rh/SiO_2$ catalyst.
(3) The surface carbon formed is hydrogenated to methane with a maximum methanation rate at 442 K during TPR on $Ag–Rh/SiO_2$.

(4) The higher methane peak temperature of 442 K on Ag–Rh/$SiO_2$ than on Rh/$SiO_2$ is due to the suppression of hydrogenation by Ag.
(5) Linear CO may be more reactive than bridged CO for methanation during TPR over both Rh/$SiO_2$ and Ag–Rh/$SiO_2$.

The experimental technique of TPR coupled with IR spectroscopy used for this study yielded information on the structure and reactivity of adsorbed CO towards hydrogen, the activation energy, and the kinetic parameters for the reaction.

## Acknowledgement

RK is grateful for the financial support from the Department of Chemical Engineering, The University of Akron.

## References

[1] J.L. Falconer and J.A. Schwarz, Catal. Rev. Sci. Eng., 25 (1983) 141.
[2] R.J. Cvetanovic and Y. Amenomiya, Catal. Rev., 6(1) (1972) 21.
[3] J.A. Schwarz, B.G. Russel and H.F. Harnsberger, J. Catal., 54 (1978) 303.
[4] G.H. Yokomizo, C. Louis and A.T. Bell, J. Catal., 120 (1989) 15.
[5] H. Miura and R.D. Gonzalez, J. Phys. E: Sci. Instrum., 15 (1982) 373.
[6] T.P. Wilson, P.H. Kasai and P.C. Ellgen, J. Catal., 69 (1981) 193.
[7] J.R. Katzer, A.W., Sleight, P. Gajarsdo, J.B. Michel, E.F. Gleason and S. McMillian, Faraday Discuss. Chem. Soc., 72 (1981) 121.
[8] F.G.A. Van den Berg, J.H.E. Glezer and W.M.H. Sachtler, J. Catal., 93 (1985) 340.
[9] S.C. Chuang, J.G. Goodwin, Jr. and I. Wender, J. Catal., 95 (1985) 435.
[10] R.P. Underwood and A.T. Bell, J. Catal., 111 (1988) 325.
[11] S.S.C. Chuang and S.I. Pien, J. Catal., 138 (1992) 536.
[12] A.C. Yang and C.W. Garland, J. Phys. Chem., 61 (1957) 1504.
[13] S.D. Worley, C.A. Rice, G.A. Mattson, C.W. Curtis, J.A. Guin and A.R. Tarrer, J. Chem. Phys., 76 (1982) 20.
[14] J.T. Yates, T.M. Duncan, S.D. Worley and R.M. Vaughan, J. Chem. Phys., 70 (1979)1219.
[15] F. Solymosi and M. Pasztor, J. Phys. Chem., 90 (1986) 5312.
[16] S. Kesraoui, R. Oukaci and D.G. Blackmond, J. Catal., 105 (1987) 432.
[17] Y.E. Li and R.D. Gonzalez, J. Phys. Chem., 92 (1988) 1589.
[18] K. Fujimoto, M. Kameyama and T. Kunugi, J. Catal., 61 (1980) 7.
[19] Y. Mori, T. Mori, A. Miyamoto, N. Takahashi, T. Hattori and Y. Murakami, J. Phys. Chem., 93 (1989) 2039.
[20] T. Mori, A. Miyamoto, H. Niizuma, N. Takahashi, T. Hattori and Y. Murakami, J. Phys. Chem., 90 (1986) 109.
[21] F. Solymosi, I. Tombacz and M. Kocsis, J. Catal., 75 (1982) 78.
[22] A. Erdohelyi and F. Solymosi, J. Catal., 84 (1983) 446.
[23] G.A. Somorjai, Catal. Rev. Sci. Eng., 23 (1981) 189.
[24] S.L. Tang, M.B. Lee, Q.Y. Yang, J.D. Beckerle and S.T. Ceyer, J. Chem. Phys., 84(3) (1986) 1876.
[25] S.S.C. Chuang, S.I. Pien and R. Narayanan, Appl. Catal., 57 (1990) 241.
[26] G. Srinivas, Ph.D. Dissertation, The University of Akron, Akron, OH 1994.
[27] R.M. Hammaker, S.A. Francis and R.P. Eichens, Spectrochem. Acta., 21 (1965) 1295.
[28] H.C. Peebles, D.D. Beck, J.M. White and C.T. Campbell, Surf. Sci., 150 (1985) 120.

[29] F. Solymosi, T. Bansagi and E. Novak, J. Catal., 112 (1988) 183.
[30] F. Solymosi and M. Pasztor, J. Phys. Chem., 89 (1985) 4789.
[31] S.S.C. Chuang, G. Srinivas and A. Mukherjee, J. Catal., 139 (1993) 490.
[32] D.W. Goodman, Heterogeneous Catalysis, Texas A&M University Press, College Station, Vol. 2, 1984, p. 230.
[33] C.M. Chan, R. Aris and W.H. Weinberg, Appl. Surf. Sci., 1 (1978) 360.
[34] E.E. Ibok and D.F. Ollis, J. Catal., 66 (1980) 391.
[35] R. Chen, Surf. Sci., 43 (1974) 657.
[36] R.J. Gorte, J. Catal., 75 (1982) 164.
[37] R. Narayanan, M.S. Thesis, The University of Akron, Akron, OH 1990.